

Shear Flow of Sea Ice in the Marginal Ice Zone with Collision Rheology

Matti Leppäranta ⁽¹⁾, Mikko Lensu ⁽¹⁾ and Qian-Ming Lu ⁽²⁾

1) Finnish Institute of Marine Research
P.O. Box 33, SF-00931 Helsinki, Finland

2) Danish Hydraulic Institute
Agern Alle 5, DK-2970 Horsholm, Denmark

Abstract

Ice edge parallel shear flow in the marginal ice zone is analysed with analytic methods. For the rheology of ice a recent ice floe collision model is used; this rheology gives a quadratic stress — strain rate law.

Analytic solution is presented for the steady state shear flow. This solution necessitates a non-zero gradient and on-ice component in the wind field. The ice velocity field is linearly related to the wind field, and the proportionality coefficient depends on the air and water drag parameters and the inelasticity or restitution coefficient of the ice floe collisions. The ice compactness profile is extremely sharp, practically a step function stepping from zero to maximum compaction at the ice edge.

The analytic solution of the velocity distribution across the marginal ice zone is rather general just assuming a constant or space-independent shear stress to normal stress ratio. It is only this ratio where the ice stress is reflected in the ice velocity field. The ice compactness profile is dictated by the form of compactness dependency in the normal stress, and the sharpness of the profile is due to the very strong non-linearity of this dependency.

1. Introduction

Sea ice fields are discrete, granular material. As one may easily observe from *e.g.* satellite imagery, a sea ice cover consists of separate individual ice floes. The size of the floes depends highly on the location: the order of magnitude of floe diameters increases from 10 m close to the open sea to 100 km in the Central Arctic Basin. Various processes continuously act within the ice pack to conserve its discrete nature (*e.g.* Rothrock, 1975).

The marginal ice zone (MIZ) is loosely defined as the zone of 100 km width in the ice pack next to the open ocean. In the MIZ the ice floes are relatively small, diameter 10 m to 1 km. The region is known to be highly active and variable, and it has

been speculated that ice floe collisions have an important role in the MIZ ice dynamics. The question has not yet been settled however.

Recently a few investigations have been made on the applicability of granular flow theories to sea ice motion in the MIZ (*Shen et al.*, 1986, 1987; *Lu*, 1988). It has been hypothesized that a system of ice floes moves like a "rapid granular flow" where momentum is transferred within the system through floe collisions, and the sink of kinetic energy is the inelasticity of the collisions. In such flow the stress within the ice, dictated by the intensity of the collisions, depends quadratically on the strain rate. Thus the collision rheology is very different from the widely used plastic sea ice models which give strain rate independent stresses (*Coon et al.*, 1974; *Hibler*, 1979). However, these plastic models are mainly based on the ice ridging process which is the main sink of kinetic energy in the Central Arctic whereas only little ridging occurs in the MIZ.

Examining ice kinematics data from the Greenland Sea, *Shen et al.* (1986) found rather good correlation in the ice velocity fluctuations between the measurements and predictions based on the collision rheology. There was, however, a large difference in the magnitude of the fluctuations. This difference could later be significantly decreased by *Lu* (1988) in his work on collision models.

In the present work the ice dynamics equations with collision rheology are investigated using analytic methods. The principal interest lies in the shear flow parallel to the ice edge in the MIZ. For such case analytic solutions of ice velocity across the MIZ are found. It is hoped that these analytic solutions of the ice dynamics problem help to identify the effect of floe collisions in real data. Earlier works lack this kind of approach. The present paper is neither a proof nor a disproof for the ice floe collision problem but aims to give tools for later considerations.

2. *Collision rheology*

2.1. Basic equation

In the present analysis ice floes are idealized as uniform size circular discs. Ice floe collisions are generated by random fluctuations in ice velocity. The frequency of the collisions depends on the magnitude of the velocity fluctuations and the compactness of ice, and the nature of the collisions is described with a restitution (or inelasticity) coefficient. The stress generated by the collisions is dictated by the rate momentum is transferred within the system and hence naturally is directly proportional to the mass of the floes. To close the system the level of the random velocity fluctuations needs to be determined. This is made through the mechanical energy equation providing the fluctuation level on the basis of energy dissipation in the deformation of the ice. Thus

the fluctuation level and stress are zero if and only if deformation is zero.

The collision rheology equation is usually expressed as (for a detailed derivation, see *Shen et al.*, 1987 or *Lu*, 1988)

$$\sigma = \rho_I h D^2 \frac{1 + \beta}{4} \frac{A^{3/2}}{\sqrt{A_0 - \sqrt{A}}} \frac{v'}{D} \left\{ \frac{2}{3\pi} (\text{tr } \dot{\epsilon} \mathbf{I} + \dot{\epsilon}) - \frac{4\sqrt{2}}{\pi^2} \frac{v'}{D} \mathbf{I} \right\} \quad (2.1)$$

where σ is the ice stress tensor, ρ_I is ice density, h is floe thickness, D is floe diameter, β is restitution coefficient ($0 \leq \beta \leq 1$), A is ice compactness, A_0 is maximum ice compactness, v' is velocity fluctuation level, $\dot{\epsilon}$ is strain rate tensor of ice, and \mathbf{I} is unit tensor.

The strain rate tensor is defined by

$$\dot{\epsilon}_{xx} = \frac{\partial u}{\partial x}, \quad \dot{\epsilon}_{xy} = \dot{\epsilon}_{yx} = \frac{1}{2} \left(\frac{\partial u}{\partial y} + \frac{\partial v}{\partial x} \right), \quad \dot{\epsilon}_{yy} = \frac{\partial v}{\partial y} \quad (2.2)$$

where u and v are the east and north components of ice velocity. The principal strain rates are

$$\dot{\epsilon}_{1,2} = \frac{1}{2} (\dot{\epsilon}_{xx} + \dot{\epsilon}_{yy}) \pm \sqrt{\frac{1}{4} (\dot{\epsilon}_{xx} - \dot{\epsilon}_{yy})^2 + \dot{\epsilon}_{xy}^2} \quad (2.3)$$

with + sign taken for $\dot{\epsilon}_1$. Convenient strain rate invariants for the present study are given by

$$\dot{\epsilon}_I = \dot{\epsilon}_1 + \dot{\epsilon}_2, \quad (2.4a)$$

$$\dot{\epsilon}_{II} = \dot{\epsilon}_1 - \dot{\epsilon}_2, \quad (2.4b)$$

equal to, respectively, rate of compression and twice the maximum rate of shear. The velocity fluctuation level v' is given by

$$\frac{v'}{D} = \sqrt{k_1^2 - k_2} - k_1 \quad (2.5a)$$

where

$$k_1 = \left[\frac{4\sqrt{2}}{\pi^2} \frac{1}{1-\beta} - \frac{2\sqrt{2}}{\pi} \right] \dot{\epsilon}_I, \quad (2.5b)$$

$$k_2 = \left[\frac{1}{4} \dot{\epsilon}_I^2 + \frac{1}{8} \dot{\epsilon}_{II}^2 \right] - \frac{8}{3\pi(1-\beta)} \left[\frac{3}{4} \dot{\epsilon}_I^2 + \frac{1}{4} \dot{\epsilon}_{II}^2 \right]. \quad (2.5c)$$

The derivation of Eq. (2.1) is based on the assumption

$$v' \gg D \sqrt{\dot{\epsilon}_I^2 + \dot{\epsilon}_{II}^2} \quad \left\{ = \sqrt{2} D \sqrt{\dot{\epsilon}_I^2 + \dot{\epsilon}_{II}^2} \right\}. \quad (2.6)$$

Through simple manipulation we see that the rheology equation (2.1) can be expressed as a Reiner-Rivlin fluid law with a pressure and shear viscous term:

$$\sigma = m(1 + \beta)g(A)[-f_1\mathbf{I} + f_2\dot{\epsilon}'] \quad (2.7)$$

where $m = \rho_I h D^2$ is ice floe mass per unit area, $g(A) = A^{3/2}/(\sqrt{A_0} - \sqrt{A})$, $\dot{\epsilon}' = \dot{\epsilon} - \frac{1}{2}\text{tr}\dot{\epsilon}\mathbf{I}$ is the deviatoric strain rate, and finally the pressure and shear viscosity factors f_1 and f_2 are given by

$$f_1 = -\frac{1}{4\pi} \cdot \frac{v'}{D} \dot{\epsilon}'_{\text{I}} + \frac{\sqrt{2}}{\pi^2} \left(\frac{v'}{D}\right)^2, \quad (2.8a)$$

$$f_2 = \frac{1}{6\pi} \frac{v'}{D}. \quad (2.8b)$$

Note that v'/D is a first-degree homogeneous function of the strain rate invariants which are here considered as state variables (*cf. Smith, 1983*). Consequently, both the pressure and the shear stress are quadratic in the strain rate.

It is seen that the ice stress depends on three parameters (ρ_I, β, A_0), floe characteristics (D, h), ice compactness, velocity fluctuations and the strain rate. The values chosen for the parameters and standard floe characteristics are shown in Table 1.

Table 1. Collision rheology parameters and standard Marginal Ice Zone (MIZ) floe characteristics.

Quantity	Value	Comments
Ice density	0.91 g cm ⁻³	Well known
Restitution coefficient β	0.9	<i>Shen et al. (1987)</i>
Maximum compactness A_0	$\pi/2\sqrt{3} \approx 0.907$	Theoretical
Floe diameter D	100 m	MIZ variation 10 m – 1 km
Floe thickness h	2 m	MIZ variation 0.5 m – 4 m

Equation (2.5) shows that the velocity fluctuation level scaled with the floe diameter depends on the strain rate invariants and the restitution coefficient. Fig. 1 shows the sensitivity of the fluctuation level to the ratio of the strain rate invariants. Here the fluctuation level has been scaled with $(\dot{\epsilon}'_{\text{I}}^2 + \dot{\epsilon}'_{\text{II}}^2)^{1/2}$; for a fixed restitution coefficient this scaled quantity depends only on the ratio $\gamma = \dot{\epsilon}'_{\text{I}}/\dot{\epsilon}'_{\text{II}}$. Note that $\gamma = 0$ corresponds to pure shear, $\gamma = +1$ or $\gamma = -1$ to uniaxial dilatation or compression, and $\gamma \rightarrow +\infty$ or $-\infty$ to pure divergence or pure convergence. Fig. 1 shows that in a diverging situation the fluctuation level is quite low and independent of the restitution coefficient

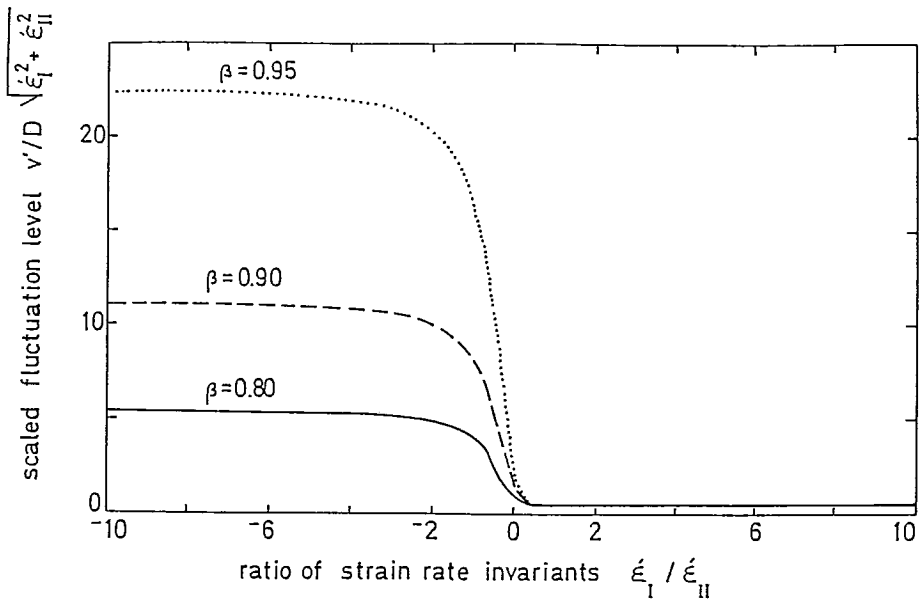


Fig. 1. The velocity fluctuation level v' as a function of the ratio of the strain rate invariants $\dot{\epsilon}_I$ and $\dot{\epsilon}_{II}$. The symbol D stands for the floe diameter and β for the restitution coefficient.

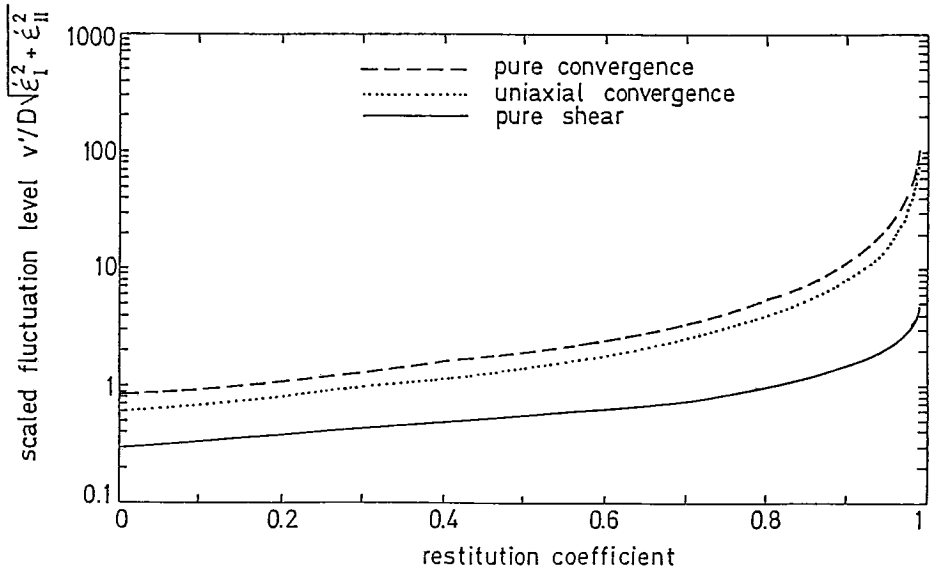


Fig. 2. The velocity fluctuation level as a function of the restitution coefficient in shear and convergence.

whereas in a converging situation the case is vice versa. As γ decreases from 0 to -2 the fluctuation level increases and then turns to nearly a constant value, and also is quite sensitive to the restitution coefficient. It is clear that the higher the restitution coefficient the higher the velocity fluctuation level since less and less kinetic energy is lost in the collisions.

The dependency of the fluctuation level on the restitution coefficient is illustrated in Fig. 2 for the convergence and shear cases. The basic assumption (2.6) for deriving the present explicit expression (2.1) of the floe collision rheology states that random displacements must be much larger than displacements caused by the strain rate field. Translating "much" to "double", Fig. 2 shows that the assumption is satisfied for $\beta \gtrsim 0.3$ in pure convergence and $\beta \gtrsim 0.9$ in pure shear. As β approaches unity then v' blows to infinity. In diverging situations the calculations gave scaled fluctuation levels less than one everywhere and thus the analytic solution should not be used then (see Fig. 1).

It is easy to see from the above formulae that the velocity fluctuation level is directly proportional to the floe diameter whereas the stress is proportional to the squared floe diameter.

Next the order of magnitude of the collision rheology stresses is considered. From *Leppäranta and Hibler* (1987) it is seen that in a rapidly deforming MIZ the characteristic strain rate is 10^{-5} s^{-1} which was chosen for the present magnitude calculations as the absolute value of the principal strain rates. Then, using Table 1 where necessary, the velocity fluctuation level and the stress were obtained for variable compactness and restitution coefficient in pure shear and in pure convergence. The results are shown in Table 2; the stress invariants are here defined similarly as the strain rate invariants (see eq. 2.4). Fig. 3 shows the dependency of the stress invariant ratio from the strain rate invariant ratio.

The predicted level of velocity fluctuations in shear flow is quite low as stated already in *Shen et al.* (1987). It is seen from *Leppäranta and Hibler* (1987) that the variance level of pure random fluctuations in ice motion is of the order of $10^{-1} \text{ cm}^{-2} \text{ s}^{-2}$ on average. For rapid flow, as the strain rate becomes 10^{-5} s^{-1} , the variance increases by two orders of magnitude. In the present numerical case the value of v' is one order of magnitude too small. In convergence the fluctuation level seems to reach a reasonable magnitude for $\beta \approx 0.9$ but much too large for $\beta > 0.9$. However, in reality pure convergence is a rare occurrence in the MIZ and typically MIZ flow is rather close to shear flow (*Leppäranta and Hibler*, 1987).

The reasons for the unnaturally low level of velocity fluctuations in shear flow are discussed in *Shen et al.* (1986). They suggest that the geometric characteristics or material properties of ice floes are not well represented in the model idealization. For more, other sources of fluctuations such as oceanic and atmospheric turbulence may

Table. 2. The magnitude of the velocity fluctuation level v' and stress invariants for some selected values of ice compactness A and restitution coefficient β . The principal strain rates are 10^{-5} s^{-1} in absolute value. Maximum compactness is 0.907.

A	β	Pure shear			Pure convergence	
		v' cm s ⁻¹	σ_I Nm ⁻¹	σ_{II} Nm ⁻¹	v' cm s ⁻¹	σ_I Nm ⁻¹
0.800	0.90	0.28	-0.098	0.013	2.22	-6
0.900	0.90	0.28	-1.862	0.244	2.22	-121
0.906	0.90	0.28	-14.425	1.889	2.22	-938
0.900	0.85	0.23	-1.172	0.192	1.46	-52
0.900	0.90	0.28	-1.862	0.244	2.22	-121
0.900	0.95	0.41	-3.942	0.360	4.52	-500
0.900	0.99	0.92	-20.606	0.834	22.86	-12818

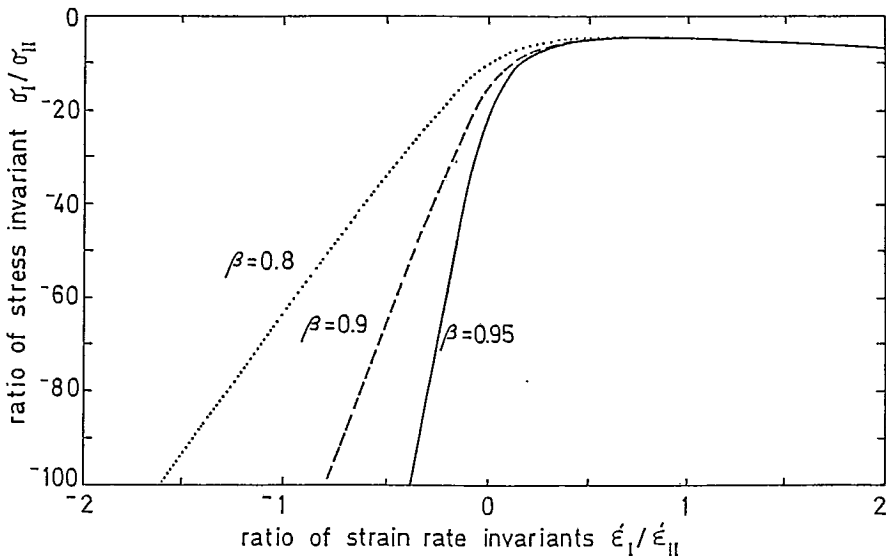


Fig. 3. The ratio of stress invariants versus the ratio of strain rate invariants for various restitution coefficients β .

cause an increased fluctuation level. Anyway, in spite of the level difference a good correlation was found by *Shen et al.* (1986) between the theory and ice kinematics observations. Later *Lu* (1988) could significantly lower the level difference through using a larger ice floe diameter.

The stresses in Table 2 are very low except for convergence in highly compact ice or with high restitution coefficient. However, as $A \rightarrow A_0$ then $\sigma \rightarrow \infty$. The singularity is in reality ruled out by the stress achieving the yield limit of ridging which is of the order of magnitude of 10^4 Nm^{-1} (e.g., *Hibler*, 1979). At this yield limit ice floes begin to override each other thus violating one of the basic assumptions of the collision rheology. In shear flow the stress is at the yield limit for $A - A_0 \sim 10^{-6}$.

2.2. Pure shear flow

In pure shear flow the only non-zero velocity derivative is $\partial v / \partial x$. The strain rate becomes

$$\begin{aligned} \dot{\epsilon}_{xx} &= 0, & \dot{\epsilon}_{xy} &= \frac{1}{2} \frac{\partial v}{\partial x}, & \dot{\epsilon}_{yy} &= 0, \\ \dot{\epsilon}_1 &= \frac{1}{2} \frac{\partial v}{\partial x}, & \dot{\epsilon}_2 &= -\frac{1}{2} \frac{\partial v}{\partial x}. \end{aligned} \quad (2.9)$$

Now $k_1 = 0$, and the velocity fluctuation level is

$$\frac{v'}{D} = c \left| \frac{\partial v}{\partial x} \right|, \quad c = \left[\frac{2}{3\pi(1-\beta)} - \frac{1}{8} \right]^{\frac{1}{2}}. \quad (2.10)$$

Note that the standard numerical value of $\beta = 0.9$ gives c equal to 1.41.

Then the ice stress is

$$\sigma_{xx} = -m(1+\beta)g(A) \cdot \frac{\sqrt{2}}{\pi^2} c^2 \left(\frac{\partial v}{\partial x} \right)^2 \quad (2.11a)$$

$$\sigma_{xy} = m(1+\beta)g(A) \cdot \frac{1}{12\pi} c \operatorname{sgn} \left(\frac{\partial v}{\partial x} \right) \left(\frac{\partial v}{\partial x} \right)^2 \quad (2.11b)$$

$$\sigma_{yy} = \sigma_{xx}. \quad (2.11c)$$

In pure shear the stress invariants are equal to $2 \cdot \sigma_{xx}$ and $2 \cdot \sigma_{xy}$ respectively. The shear stress is directly proportional to the normal stress, i.e.

$$|\sigma_{II}|/|\sigma_I| = \kappa = \frac{\pi}{12\sqrt{2}c}. \quad (2.12)$$

Thus in pure shear flow the normal stress is one order of magnitude larger than the shear stress. According to the present understanding of ice dynamics this difference

is too much. There is some evidence based on observations (*e.g.*, Hibler and Tucker, 1979) that the stress ratio κ should be of the order of 0.5. However, these pieces of evidence are far from the marginal ice zone. In the collision rheology the stress ratio depends only on the restitution coefficient β ; $\kappa = 0.191$ for $\beta = 0.8$, $\kappa = 0.131$ for $\beta = 0.9$, and $\kappa \rightarrow 0$ as $\beta \rightarrow 1$.

2.3. Convergence

In pure convergence the principal strain rates are equal and negative. As the strain rate also the stress tensor is spherical, and the diagonal components are

$$\sigma_{xx} = \sigma_{yy} \propto m(1 + \beta)g(A)\dot{\epsilon}_{xx}^2, \quad (2.13)$$

where the proportionality factor is, *e.g.*, 0.0062 for $\beta = 0.9$.

In uniaxial convergence the principal strain rates are $\dot{\epsilon}_1 = 0$ and $\dot{\epsilon}_2 = \dot{\epsilon}_{xx} < 0$. The stresses become

$$\sigma_{xx} \propto m(1 + \beta)g(A)\dot{\epsilon}_{xx}^2 \quad (2.14a)$$

$$\sigma_{xy} \propto m(1 + \beta)g(A)\dot{\epsilon}_{xx}^2 \quad (2.14b)$$

$$\sigma_{yy} \propto m(1 + \beta)g(A)\dot{\epsilon}_{xx}^2 \quad (2.14c)$$

The proportionality factors when $\beta = 0.9$ are 0.0146, -0.0464 and -0.0162 in Eqs. (2.14a, b and c), respectively. Here the stress components are directly proportional to each other with the proportionality factor depending on the restitution coefficient. The shear to normal stress invariant ratio is $\sigma_{II}/\sigma_I = -0.021$.

The convergent cases are not so interesting because of their transience. During convergence ice compactness increases which steadily tends to increase the stress level. To compensate this all movement must slow down, and the limiting steady state solution is immobile ice pack.

3. Ice dynamics model for shear flow

3.1. Basic equations

We consider here a purely dynamic model for the motion of ice. The momentum equation includes the inertial term, Coriolis term, ice stress, and the air and water stresses on the top and bottom surfaces of the ice. Geostrophic ocean currents are neglected. Since in the collision model ice floes are not allowed to override on each other, ice

mass changes appear only in the compactness of ice. With these simplifications the momentum and continuity equations become (from, *e.g.*, Hibler, 1986)

$$\rho_I h \left(\frac{d\bar{u}}{dt} + f \hat{k} \times \bar{u} \right) = \nabla \cdot \sigma + \bar{\tau}_a + \bar{\tau}_w, \quad (3.1)$$

$$-\frac{\partial A}{\partial t} = -\nabla \cdot (\bar{u}A), \quad (3.2)$$

where d/dt is the material time derivative, f is Coriolis parameter, \hat{k} is the unit vector vertically upward, and $\bar{\tau}_a$ and $\bar{\tau}_w$ are the air and water stresses. The air and water stresses are generally determined from (*e.g.*, Brown, 1980; McPhee, 1982),

$$\bar{\tau}_a = \rho_a C_a \bar{U}_a \left(\cos \phi + \sin \phi \hat{k} \times \right) \bar{U}_a, \quad (3.3)$$

$$\bar{\tau}_w = \rho_w C_w |\bar{U}_w - \bar{u}| \left(\cos \theta + \sin \theta \hat{k} \times \right) (\bar{U}_w - \bar{u}), \quad (3.4)$$

where for air and water, respectively, ρ_a and ρ_w are densities, C_a and C_w are drag coefficients, \bar{U}_a and \bar{U}_w are geostrophic velocities, and ϕ and θ are turning angles. Here the geostrophic water velocity is assumed zero.

3.2. Marginal ice zone (MIZ)

For the marginal ice zone, shear flow parallel to the ice edge is of particular interest. External conditions in the air and sea favour such MIZ shear flows to develop.

The present idealized configuration for the MIZ is shown in Fig. 4. The y -axis is aligned parallel to the MIZ and defines the ice edge. The system is assumed invariant in the direction of the MIZ. The length scale of the MIZ width is usually referred to as 100 km. This scale is physically dictated by the ice strength and external forcing. In the MIZ ice deformation is mostly opening and closing the packing of ice floes since the stress within the ice does not achieve the yield stress for ridge build-up σ_* . Taking the wind stress as the governing external force, the MIZ width scale L is obtained from

$$\tau_{ax} L \sim \sigma_*. \quad (3.5)$$

Since $\tau_{ax} \sim 10^{-1} \text{ Nm}^{-2}$ and $\sigma_* \sim 10^4 \text{ Nm}^{-1}$ (see Hibler, 1986), we have $L \sim 100 \text{ km}$.

In steady state MIZ flow u -velocity must be identically zero. Then the continuity equation (3.2) is automatically satisfied, and the momentum equation becomes

$$\frac{d}{dx} \sigma_{xx} + \tau_{ax} + \rho_w C_w \sin \theta \text{sgn}(v) v^2 + \rho_I h f v = 0 \quad (3.6)$$

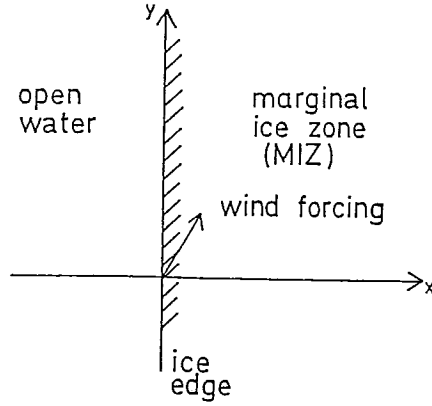


Fig. 4. Idealized marginal ice zone.

$$\frac{d}{dx} \sigma_{xy} + \tau_{ay} - \rho_w C_w \cos \theta \operatorname{sgn}(v) v^2 = 0 \quad (3.7)$$

These two equations give the solution for the steady state distribution of the velocity and compactness of ice across the MIZ. Two boundary conditions are needed. These are chosen here through specifying the stress at the ice edge:

$$\sigma = \sigma_0, \quad x = 0 \quad (3.8)$$

Two special cases arise: 1) free ice edge with no stress ($\sigma_0 = 0$), and 2) normal stress component equal to the radiation pressure of ocean waves and zero shear component ($\sigma_{0xx} \neq 0, \sigma_{0xy} = 0$).

We now further simplify the situation through neglecting the Coriolis and turning angle effects, i.e. $f = 0$ and $\theta = 0$. This is not a serious restriction because these effects only cause a slight modification to the solution. In principle it would be quite straightforward to obtain the solution with the Coriolis and turning angle effects included as discussed later. This simplification implies that everything is symmetric with respect to the x-axis, and we can hence assume that the y-components of the forcing and velocity are positive. Then one obtains directly the solution for the stress and velocity

$$\begin{aligned} \sigma_{xx} &= - \int_0^x \tau_{ax} dx' - \sigma_{0xx} \\ v &= \left[\frac{1}{\rho_w C_w} (\tau_{ay} - \kappa \tau_{ax}) \right]^{\frac{1}{2}} \end{aligned} \quad (3.9)$$

Since v must here be positive, we must have $\tau_{ay}/\tau_{ax} > \kappa$. If this is not the case then the steady state solution is immobile ice pack.

The limiting case $\bar{\tau}_a = \text{constant}$ is not a valid solution since then $v = \text{constant}$ and hence (see Eq. 2.11) σ must be zero everywhere. Therefore we take a linear wind stress across the MIZ of width L :

$$\bar{\tau}_a = \left(1 - \frac{x}{L}\right) \bar{\tau}_{a0} \quad (3.10)$$

where $\bar{\tau}_{a0}$ is the wind stress at the ice edge. Then the normal stress becomes

$$\sigma_{xx} = -x \left(1 - \frac{1}{2} \frac{x}{L}\right) \tau_{a0x} - \sigma_{0xx} \quad (3.11)$$

Now v is of course linear across the MIZ, and from Eqs. (3.9) and (3.10)

$$\frac{dv}{dx} = -\frac{v_0^2}{vL} \quad (3.12)$$

where v_0 is the velocity at the ice edge. Ice compactness distribution is then obtained using Eqs.(2.11a and 3.11–12):

$$A^{\frac{3}{2}} + F(x)A^{\frac{1}{2}} - F(x)A_0^{\frac{1}{2}} = 0 \quad (3.13)$$

where $F(x)$ is defined by

$$F(x) = \left\{ m(1 + \beta) \frac{\sqrt{2}}{\pi^2} c^2 \left(\frac{v_0}{vL}\right)^2 \right\}^{-1} \left\{ \int_0^x \tau_{ax} dx' + \sigma_{0xx} \right\} \quad (3.14)$$

Note that a solution A with $0 \leq A \leq A_0$ exists for all $F(x) \geq 0$ such that $A = 0$ for $F(x) = 0$ and $A \rightarrow A_0$ as $F(x) \rightarrow \infty$. The solution gives an extremely sharp ice edge compactness profile (Fig. 6).

The case $\bar{\tau}_a = \text{constant}$ is approached as $L \rightarrow \infty$. Then $v \rightarrow \text{constant}$ and $A \rightarrow$ a step function with step 0 to A_0 at the ice edge.

The free ice drift solution for v -velocity is $v_f = \sqrt{\tau_{ay}/\rho_w C_w}$ and hence now

$$v/v_f = \sqrt{1 - \kappa \tan \vartheta} \quad (3.15)$$

where ϑ is the direction of wind vector relative to the ice edge (positive on-ice). This reduction is not drastic since at $\vartheta = 30^\circ$, 45° or 60° the collision model velocity is 96, 93 or 88 per cent, respectively, of the free drift. However, for u -velocity the situation is quite different because free drift cannot force the on-ice motion to stop.

Equation (3.11) gives $\sigma(L) = -\frac{1}{2}\tau_{ax}L - \sigma_{0xx}$. To keep the stress beneath the yield limit of ridging we must have

$$L < 2 \frac{|\sigma_{0xx}| - \sigma_*}{\tau_{a0x}}. \tag{3.16}$$

Selected solutions for the ice velocity and compactness profiles are shown in Figs. 5-6. Three cases are considered (Table 3). In all cases the MIZ width is 100 km and ice floe thickness 2.0 m, and the wind field is linearly ramped across the MIZ.

Table. 3. The selected shear flow cases for numerical examinations. U_a and V_a are the east and north components of the wind velocity vector, given in m/s.

	At ice edge		100 km from ice edge	
	U_a	V_a	U_a	V_a
Case 1	10	17	0	0
Case 2	3	20	0	0
Case 3	10	17	5	8.5

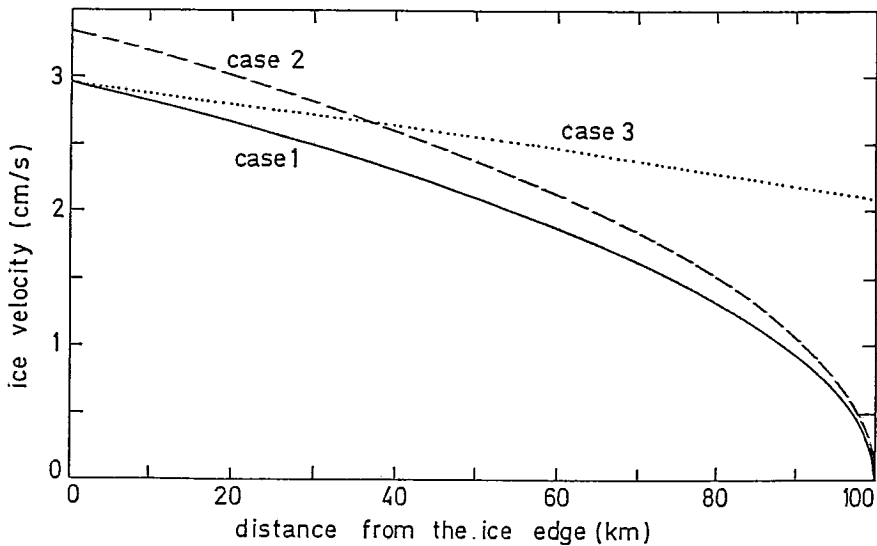


Fig. 5. Ice velocity distribution in the steady shear flow case.

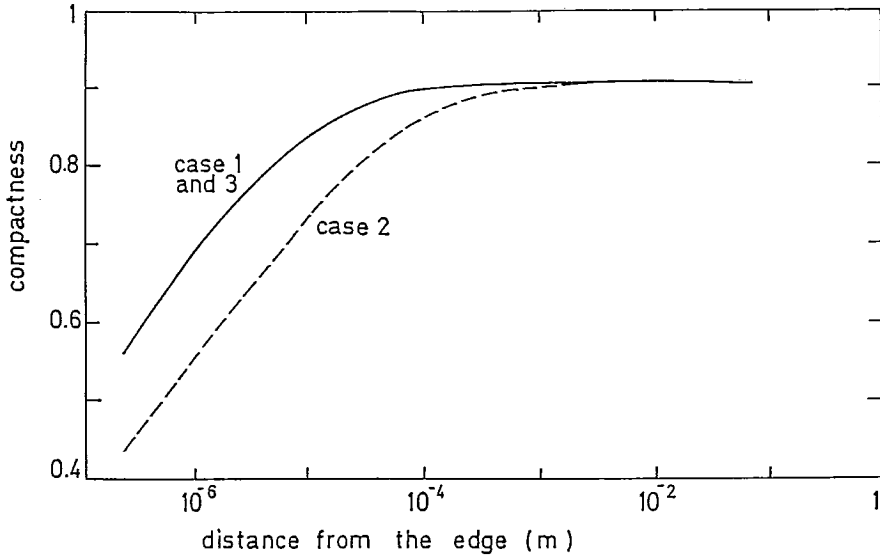


Fig. 6. Ice compactness distribution in the steady shear flow case.

At the ice edge the wind speed is 20 m/s and wind direction 30 degrees (cases 1 and 3) or 10 degrees (case 2) on-ice. The ramping goes linearly in both components to zero (cases 1 and 2) or half (case 3). The velocity profile (Fig. 5) also becomes quite linear except for rapid fall-off to zero in cases 1 and 2 close to 100 km from the ice edge where the wind has dropped off.

The ice compactness profile is extremely sharp (Fig. 6). *E.g.*, in case 2 at a distance of 1 m (much smaller than the floe diameter) the compactness deviates from the maximum of A_0 by less than 10^{-3} . In the other cases the profile is essentially similar. Therefore, the collision rheology predicts a practically rectangular compactness profile across the MIZ in the case of pure shear flow.

3.3. Wave radiation pressure effects

According to *Wadhams* (1980) the wave radiation pressure force per unit length on the ice edge is for the normal incidence of waves given by

$$\sigma_w = \frac{1}{4} \rho_w g (R_i^2 + R_r^2 - R_t^2) \quad (3.17)$$

where R_i , R_r and R_t are the amplitudes of the incoming, reflected and transmitted

waves, respectively. When there is no dissipation, i.e. $R_i^2 = R_r^2 + R_t^2$, we have

$$\sigma_w = \frac{1}{2} \rho_w g r R_i^2 \quad (3.18)$$

where

$$r = R_r^2 / R_i^2 \quad (3.19)$$

is the reflection coefficient. The wave pressure is thus proportional to the energy of the penetrating waves and the reflection coefficient, which in turn is dependent on the parameters of the waves and the properties of the ice edge. The value of r lies between 10^{-3} and 10^{-1} for typical conditions and is in general smaller for long waves which also usually are more energetic (see *Wadhams*, 1986). This means that the variable terms in (3.18) tend to compensate each other keeping the wave stress well below the strength of the ice floe field.

Taken as a boundary condition the wave pressure sharpens the compactness profile by increasing the coefficients of $F(x)$ in 3.13. Since $F(x)$ does not vanish at $x = 0$ we have a discontinuous compactness profile with a step from 0 to some minimum value $A(0)$ which for typical values of σ_w is very near A_0 .

The amplitude of the penetrated waves traveling through the floe field is attenuated according to an exponential law depending on the reflection coefficient and the geometry of the floe field (*Wadhams*, 1986). This induces an exponentially decreasing stress field into the marginal ice zone which can be used in the analytical shear flow model instead of the on-ice wind component, resulting into an exponential velocity profile and a non-vanishing compactness at the ice edge.

By using the relation $R_i = \lambda/30$ for the maximum amplitude of a wave with wavelength λ we obtain the relation $\sigma_w = 13rT^4$ for the maximum possible stress. Taking the upper limits of the reflection coefficient for waves with period $T = 10$ s and $T = 20$ s to be respectively 0.01 and 0.001, the corresponding stress limits are 10^3 and $2 \cdot 10^3 \text{ Nm}^{-1}$, i.e. one order of magnitude smaller than σ_* . However, it has been observed that ocean swell may cause ice pile-up in the very ice edge (*Bauer and Martin*, 1980), but the mechanism behind this phenomenon is apparently different from ordinary ridge formation resulting from stresses exceeding σ_* .

3.4. Extension of the basic model

The steady state solution of ice velocity and compactness for shear flow has been obtained in section 3.2.

It is interesting to note that the solution for v -velocity depends on the rheology only through the parameter κ . This constant describes the ratio between the shear and

normal stresses (see Eq. 2.12). It is not difficult to see that the solution holds for any rheology which has a constant shear to normal stress ratio. For example, the analytic plastic MIZ flow solution of *Leppäranta and Hibler (1985)* is exactly the same as here (for the same ratio κ). In the plastic model κ is a given constant parameter whereas in the collision model κ depends on the restitution coefficient.

A major feature of the collision model is that externally caused strain rates gives rise to floe collisions through random velocity fluctuations. The magnitude of these velocity fluctuations is dictated by the strain rate through mechanical energy arguments. It would be a new feature of the model to allow other sources of fluctuations raise the fluctuation level. Then the level would also be more close to observations. As other sources of fluctuations probably atmospheric and oceanic turbulence are dominant.

Adding the Coriolis and turning angle effects to the solution is straight forward. In fact, one may proceed using the plastic model results of *Leppäranta and Hibler (1985)*. For the northward v -velocity solution, then

$$v = \left[\frac{\tau_{a_y} - \kappa \tau_{a_x}}{C_*} + \left(\frac{r}{C_*} \right)^2 \right]^{\frac{1}{2}} - \frac{r}{C_*}, \quad (3.20)$$

where

$$C_* = \rho_w C_w (\cos \theta + \kappa \sin \theta), \quad (3.21)$$

$$r = \frac{1}{2} \kappa \rho_I h f. \quad (3.22)$$

Here, of course v must be positive; other solutions are taken as zero. The main implication of the Coriolis and turning angle effects is that the non-rotating case is turned to the right of the wind some 20-30 degrees or so. The condition for the mobility of the ice is that the quantity under the square root sign must be positive.

4. Conclusions

In this work ice edge parallel shear flow in the marginal ice zone (MIZ) has been analysed with analytic methods. The ice flow has been assumed as a rapid granular flow where momentum is transferred within the system through ice floe collisions. The following conclusions are presented.

1. This collision rheology, used first for sea ice by *Shen et al. (1986)*, gives a Reiner-Rivlin fluid type viscous stress law with pressure term and shear viscosity depending on the strain rate invariants and inelasticity of the collisions. The stress-strain rate law is quadratic. The stresses generated by the collisions are low except when the ice compactness is extremely close to the maximum compaction.

2. For sea ice fields, the collision model should go best in the MIZ because there only little ridging or floe overriding occurs. The width of the MIZ where ice stresses are beneath the yield limit of ridging is of the order of 100 km. However, ice floe collisions likely have a minor role in MIZ ice dynamics due to the low stress level they generate.

3. Analytic solution has been obtained here for steady shear flow parallel to the ice edge with the collision model for the stress field within the ice pack. There must be a non-zero gradient and on-ice component in the wind field for the steady state shear flow to exist. The ice velocity is linearly related to the wind velocity and deviates from the free drift by a factor which depends on the direction of the wind relative to the ice edge. When the wind direction is within 30 degrees from the ice edge direction the collision model predicts ice velocity which differs by less than 5 % from the free drift. The ice compactness profile is extremely sharp, practically a function stepping from zero to the maximum compaction at the ice edge.

4. The radiation pressure of the ocean waves to the ice edge has a very small effect on the steady state situation: the ice velocity is unchanged and the compactness profile, which already is very sharp, becomes a bit more sharpened. However, the wave pressure may have importance through keeping the ice edge together if the on-ice wind component was lacking.

5. The velocity solution is in fact rather general. It assumes that, in shear flow, the ratio of shear stress to compressive stress is a constant or at least space-independent. Then the ice interaction affects the velocity only through this stress ratio. Consequently, the steady state solution is the same in the collision model as in widely used plastic sea ice models (*Leppäranta and Hibler, 1985*). The non-steady case, on the contrary, is expected to be highly sensitive to the form of the rheology.

Further research of the collision model is recommended to consider at least two aspects. First, the time evolution for the present steady state MIZ flow solutions needs to be examined using a numerical model. The adjustment of the plastic sea ice model is slow, several days (*Leppäranta and Hibler, 1985*) whereas, by intuition, the collision model should adjust rapidly.

The second aspect is the generation mechanism for the random ice velocity fluctuations. In the present model the level of fluctuations is dictated by the ice deformation field through mechanical energy balance. The fluctuations could be thought to be generated through oceanic and atmospheric turbulence, variations in the size and form of ice floes, etc., and consequently such forcing should be added to the energy budget.

5. *References*

- Bauer, J. and S. Martin, 1980: Field observations of the Bering Sea ice edge properties during March 1979. *Mon. Wea. Rev.*, 108(12), 2045–2056.
- Brown, R.A., 1980: Boundary layer modeling for AIDJEX. In: R.S. Pritchard (ed.), *Sea Ice Processes and Models*, pp. 387–401. University of Washington Press, Seattle.
- Coon, M.D., G.A. Maykut, R.S. Pritchard, D.A. Rothrock and A.S. Thorndike, 1974: Modeling the pack ice as an elastic-plastic material. *AIDJEX Bulletin* 24, 1–105.
- Hibler, W.D., III, 1979: A dynamic thermodynamic sea ice model. *J. Phys. Oceanogr.*, 9, 815–846.
- Hibler, W.D., III, 1986: Ice dynamics. In: N. Untersteiner, (ed.), *Geophysics of Sea Ice*, pp. 577–640. Plenum Press, New York.
- Hibler, W.D., III and W.B. Tucker, 1979: Some results from a linear-viscous model of the Arctic ice cover. *J. Glaciol.*, 22, 293–304.
- Leppäranta, M. and W.D. Hibler III, 1985: The role of plastic ice interaction in marginal ice zone dynamics. *J. Geophys. Res.*, 90, 11899–11909.
- Leppäranta, M. and W.D. Hibler III, 1987: Mesoscale sea ice deformation in the East Greenland marginal ice zone. *J. Geophys. Res.*, 92, 7060–7070.
- Lu, Qian-ming, 1988: On mesoscale modelling of the dynamics and thermodynamics of sea ice. Institute of Hydrodynamics and Hydraulic Engineering, Technical University of Denmark, Series Paper No. 44, 154 p.
- McPhee, M.G., 1982: Sea ice drag laws and simple boundary layer concepts, including application to rapid melting. Rep. 82-4. U.S. Army Cold Regions Research and Engineering Laboratory, Hanover, N.H.
- Rothrock, D.A., 1975: The mechanical behaviour of pack ice. *Ann. Rev. Earth Planet Sci.*, 3, 317–342.
- Shen, H.H., W.D. Hibler III and M. Leppäranta, 1986: On applying granular flow theory to a deforming broken ice field. *Acta Mechanica*, 63, 143–160.
- Shen, H.H., W.D. Hibler III and M. Leppäranta, 1987: The role of floe collisions in sea ice rheology. *J. Geophys. Res.*, 92, 7085–7096.
- Smith, R.B., 1983: A note on the constitutive law for sea ice. *J. Glaciol.*, 29(101), 191–195.
- Wadhams, P., 1980: Ice characteristics in the seasonal sea ice zone. *Cold Regions Science and Technology*, 2, 37–87.
- Wadhams, P., 1986: The seasonal ice zone. In: N. Untersteiner, (ed.), *Geophysics of Sea Ice*, pp. 825–991. Plenum Press, New York.